Journal of Colloid and Interface Science 406 (2013) 231–237

Contents lists available at SciVerse ScienceDirect

Journal of Colloid and Interface Science

www.elsevier.com/locate/jcis

A novel glucose biosensor platform based on Ag@AuNPs modified graphene oxide nanocomposite and SERS application

Vinod Kumar Gupta [a,b,*], Necip Atar [c], Mehmet Lütfi Yola [d,e], Merve Eryılmaz [f], Hilal Torul [f], Uğur Tamer [f], İsmail Hakkı Boyacı [g], Zafer Üstündağ [c]

[a] Department of Chemistry, Indian Institute of Technology Roorkee, Roorkee 247 667, India
[b] Dr. RML Avadh University, Faizabad 224 001, UP, India
[c] Dumlupinar University, Faculty of Arts and Science, Department of Chemistry, Kutahya, Turkey
[d] Sinop University, Faculty of Arts and Science, Department of Chemistry, Sinop, Turkey
[e] Hacettepe University, Faculty of Pharmacy, Department of Analytical Chemistry, Ankara, Turkey
[f] Gazi University, Faculty of Pharmacy, Department of Analytical Chemistry, Ankara, Turkey
[g] Hacettepe University, Faculty of Engineering, Department of Food Engineering, Ankara, Turkey

ARTICLE INFO

Article history:
Received 30 April 2013
Accepted 3 June 2013
Available online 13 June 2013

Keywords:
Graphene oxide
Ag@AuNPs
Characterization
Glucose biosensor
SERS

ABSTRACT

This study represents a novel template demonstration of a glucose biosensor based on mercaptophenyl boronic acid (MBA) terminated Ag@AuNPs/graphene oxide (Ag@AuNPs–GO) nanomaterials. The nanocomposites were characterized by transmission electron microscopy (TEM), X-ray photoelectron spectroscopy (XPS), and X-ray diffraction (XRD) method. The TEM image shows that Ag@AuNPs in the nanocomposite is in the range of diameters of 10–20 nm. The nanocomposite was used for the determination of glucose through the complexation between boronic acid and diol groups of glucose. Thus, a novel glucose biosensor was further fabricated by immobilizing glucose oxidase (GOD) into MBA terminated Ag@AuNPs–GO nanocomposite film (MBA–Ag@AuNPs–GO). The linearity range of glucose was obtained as 2–6 mM with detection limit of 0.33 mM. The developed biosensor was also applied successfully for the determination of glucose in blood samples. The concentration value of glucose in blood samples was calculated to be 1.97 ± 0.002 mM from measurements repeated for six times.

1. Introduction

Because of the importance of determination of glucose and decreasing of complications in diabetes patients, important researches have been performed for clinical purposes [1–8]. Nevertheless, many materials such as acetaminophen, uric acid, and ascorbic acid can interfere with the determination of glucose. In addition, a large amount of sample volume is needed for glucose determination. So, the simpler and cheaper methods can be significant in terms of clinical benefit.

Surface-enhanced Raman spectroscopy (SERS), which is based on the enhancement of Raman signal on different surfaces, is an important method because it is highly sensitive, time-saving, and widely applicable [9–13]. Several studies about the determination of glucose on SERS were reported [14–16]. For instance, Peltier et al. developed the SERS biosensor based on the zone of electromagnetic field enhancement [17], and the SERS sensor was designed on alkane-thiolate tri(ethylene glycol) monolayer [18]. Dinish et al. developed a SERS substrate with nanostructures fabricated on silicon wafer using a deep UV lithography for glucose sensing [19]. Mattei et al. prepared a SERS-active silver surface based on the action of a chemical-etching solution containing the ionic or molecular species [20]. Oh et al. developed a novel SERS substrate of glass nanopillar arrays with nanogap-rich silver nanoislands at wafer level [21]. Cejkova et al. developed copper SERS-active substrates [22]. Costa et al. investigated SERS on copper electrodes in 1-n-butyl-3-methylimidazolium tetrafluoroborate [23]. In addition, colloidal suspensions of silver and gold nanoparticles were successfully synthesized by laser ablation using water as the solvent, and excellent SERS results were found on Au films [24]. Baniukevic et al. described a magnetic gold nanoparticle in SERS-based sandwich immunoassay for BLV antigen gp51 detection using different specific antibody immobilization methods [25].

Nanocomposites have aroused extensive interest due to thermal, chemical, physical, and catalytic properties [26]. Because of the large surface area, graphene/graphene oxide has been an attractive nanomaterial [27]. Hence, there are many reports about composites which integrate graphene oxide or graphene with different nanoscaled materials [28]. Among them, metal–graphene nanocomposites are very useful for various engineering

* Corresponding author at: Department of Chemistry, Indian Institute of Technology Roorkee, Roorkee 247 667, India. Fax: +91 1332273560/36.
E-mail addresses: vinodfcy@iitr.ernet.in, vinodfcy@gmail.com (V.K. Gupta).

0021-9797/$ - see front matter © 2013 Elsevier Inc. All rights reserved.
http://dx.doi.org/10.1016/j.jcis.2013.06.007

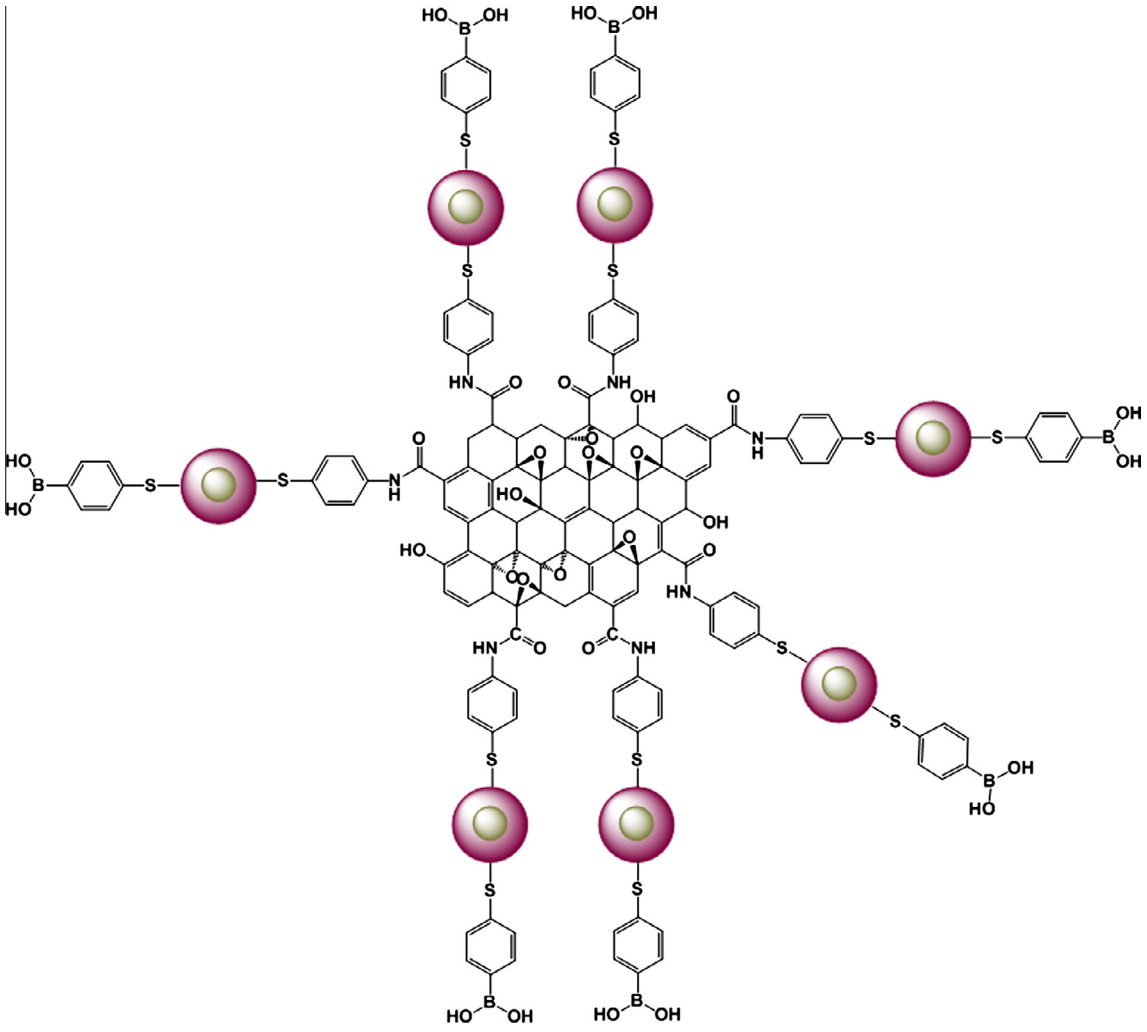

Scheme 1. The proposed structure of MBA–Ag@AuNPs–GO nanocomposite.

applications such as fuel cell catalysis [29–31], batteries [32,33], production of hydrogen [34,35], semiconductor photocatalysts [36,37], and drug delivery and biosensors [38–42]. The reason for this widespread use is electrochemically active surface areas with metal–graphene nanocomposites, and hence, a more rapid and sensitive current response between electrode and target molecules is provided.

In this study, a glucose determination is performed using SERS, which is based on a novel MBA–Ag@AuNPs–GO nanocomposite. We report a facile, cost-effective, and environmentally friendly method. The proposed structure of the synthesized MBA–Ag@AuNPs–GO nanocomposite is shown in Scheme 1. The MBA–Ag@AuNPs–GO nanocomposite shows excellent SERS activity as SERS substrates. Further, when GOD was immobilized into MBA–Ag@AuNPs–GO nanocomposite film, the SERS substrates showed appropriate linear range for determination of glucose. More importantly, the developed SERS substrates were applied to human blood serum for determination of glucose.

2. Experimental

2.1. Reagents

Graphite powder (Sigma–Aldrich), hydrogen tetrachloroaurate hydrate ($HAuCl_4$) (Sigma–Aldrich), β-Cyclodextrin (β-CD), Silver nitrate ($AgNO_3$), p-aminothiophenol (ATP) (Sigma–Aldrich), trisodium citrate dihydrate ($Na_3C_6H_5O_7{\cdot}2H_2O$) (Sigma–Aldrich), 1-ethyl-3-[3-dimethylaminopropyl] carbodiimide hydrochloride (EDC) (Sigma–Aldrich), hydrogen peroxide (H_2O_2) (Merck), potassium permanganate ($KMnO_4$) (Merck), sulfuric acid (H_2SO_4) (Merck), and other chemicals were of reagent grade quality. GOD (100–250 units/mg from *Aspergillus niger*) and bovine serum albumin (BSA) were purchased from Sigma–Aldrich. Human serum albumin (HSA), complement III (C3), and transferrin were supplied from the Central Institute of Hygiene in Turkey (Ankara). Glucose stock solutions were stored at room temperature before use. All the experiments in aqueous media were performed with ultra pure quality water.

2.2. Instrumentation

DeltaNu Examiner Raman Microscopy system (Deltanu Inc., Laramie, WY) with a 785 nm laser source, a motorized microscope stage sample holder, and a cooled charge-coupled device (CCD, at 0 °C) detector was used to detect GOD. The instrument parameters were as follows: 20× objective, laser spot size of 30 mm, laser power of 150 mW, and acquisition time of 50 s. Baseline correction was performed for all of the measurements.

TEM measurements were performed with a JEOL 2100 HRTEM instrument (JEOL Ltd., Tokyo, Japan) to examine the morphology of graphene oxide and Ag@AuNPs–GO.

An ES300 electron spectrometer with Mg Kα X-rays was used for XPS measurements, which were performed at 90° electron

take-off angle. The pressure was maintained at 10^{-7} Pa. The sample for XPS measurement was prepared on a clean glass slide by placing one drop of the nanostructure and then allowing them to dry in air.

A Rikagu Miniflex X-ray diffractometer using monochromatic Cu Kα radiation operating at a voltage of 30 kV and current of 15 mA was used for X-ray diffraction measurements of the nanocomposites. A scanning speed of 2° 2θ/min and a step size of 0.02° were used to examine the samples in the range of 5–75° 2θ.

2.3. Preparation of AgNPs and Ag@AuNPs

The initial silver colloids were synthesized according to the following procedure [43]. $AgNO_3$ was reduced by β-CD in aqueous media. The reaction mixture was heated until the color of solution converted into pale yellow. The color of pale yellow indicated the formation of silver nanoparticles (AgNPs). After that, $HAuCl_4$ solution (1 mM) was added to the colloidal silver solution for the preparation of Ag@AuNPs. Then, the solution was incubated for 15 min at room temperature. After incubation, the solution was heated on a water bath. The color of solution was changed from pale yellow to pink, which indicates the formation of Ag@AuNPs.

2.4. Preparation of GO

GO was synthesized according to modified Hummers method [44–46]. A mixture containing 25 mL of H_2SO_4 (98%), 5 g of $K_2S_2O_8$, 5 g of P_2O_5, and 5 g of graphite powder was placed in a flask and was kept at 80 °C for 6 h. The mixture was cooled to 20 °C and diluted with ultra pure 1 L water and left for 12 h. The pre-oxidized carbon material was filtered and washed with ultra pure water. The pre-treated graphite was diluted with 250 mL of H_2SO_4 (98%) at 0 °C. 30 g of $KMnO_4$ was added in the suspension and cooled to 20 °C. After the $KMnO_4$ saturation, the flask was heated to about 35 °C. The mixture was stirred at this temperature for 4 h and then diluted with 500 mL of ultra pure water in the ice bath. The resulting mixture was stirred for 2 h. The mixture was diluted with 2 L of ultra pure water. Then, the suspension was treated with 40 mL of H_2O_2 (30%). The color of the suspension changed from brownish to brilliant yellow, and the mixture was stirred until the end of the bubbling. The synthesized GO was filtered and washed with 0.1 M HCl and ultra pure water three times, respectively. The GO was precipitated by using an ultracentrifuge and dried under the atmospheric air conditions.

2.5. Preparation of Ag@AuNPs–GO and MBA–Ag@AuNPs–GO composite

The synthesized GO was dissolved in ethanol with the aid of ultrasonic agitation for 1 h, resulting in a homogeneous black suspension (2 mg mL^{-1} GO). To ensure the surface activation of carboxylate groups of GO, the GO suspension was allowed to react with 0.2 M EDC solution for 8 h. The activated GO suspension was mixed well with 1.0 mM ATP at 1:1 volume ratio for 2 h. In a typical experiment of self-assembly, the aqueous dispersion of Ag@AuNPs (1 mg mL^{-1}) was mixed with the aqueous dispersion of ATP functionalized GO (0.1 mg mL^{-1}) at a 1:1 volume ratio and sonicated for 15 min to form a homogeneous mixture. The mixture was then kept undisturbed under ambient condition for 12 h (Ag@AuNPs–GO). The self-assembled monolayer MBA–Ag@AuNPs–GO composite was formed by adding MBA (20 mM) solution on Ag@AuNPs–GO nanocomposite at a 1:1 volume ratio for 30 min.

2.6. Detection of glucose using SERS

GOD aqueous solutions with various concentrations (2.0–6.0 mM) were immobilized into MBA–Ag@AuNPs–GO nanocomposite on the surface of glass slide for 15 min. The average value of SERS spectra for B–O peak was obtained. The Raman spectra corresponding to each concentration of the GOD were recorded. The band intensity at 1070 cm^{-1} versus the GOD concentration was plotted. The data of calibration equation were calculated from the calibration curve.

3. Results and discussion

3.1. Characterizations of the nanocomposites

The morphologies of the GO and the Ag@AuNPs–GO nanocomposites were investigated using the JEOL 2100 HRTEM at an accelerating voltage of 200 keV. A drop of sample was deposited on a polymeric grid dried at room temperature under an argon gas stream. TEM images of the GO and the Ag@AuNPs–GO nanocomposites are shown in Fig. 1a and b, respectively. As shown in Fig. 1a, the TEM image of the GO appears pellucid and creased. This image exhibits its mono- or multi-layer planar sheet-like morphology. As shown in Fig. 2b, Ag@AuNPs nanocomposite has been seen as dark dots with a mean diameter of 10–20 nm on a lighter shaded substrate corresponding to the planar GO sheet.

To show attachment of Ag@AuNPs with MBA junction on the GO, XPS experiments were performed and the narrow region XPS

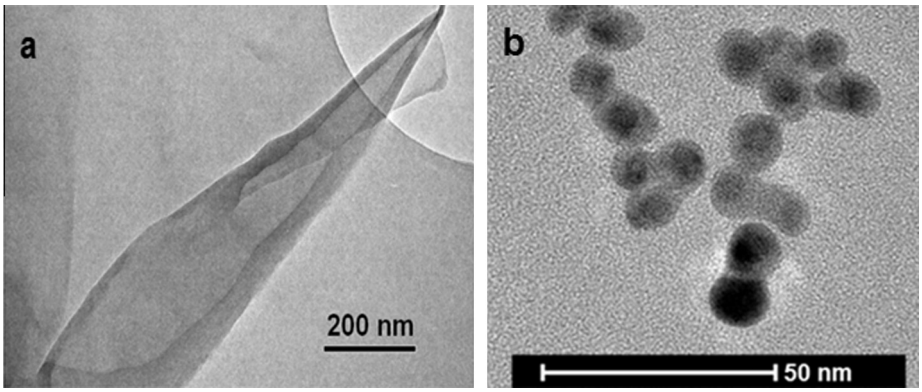

Fig. 1. TEM images of (a) GO and (b) Ag@AuNPs–GO nanocomposites.

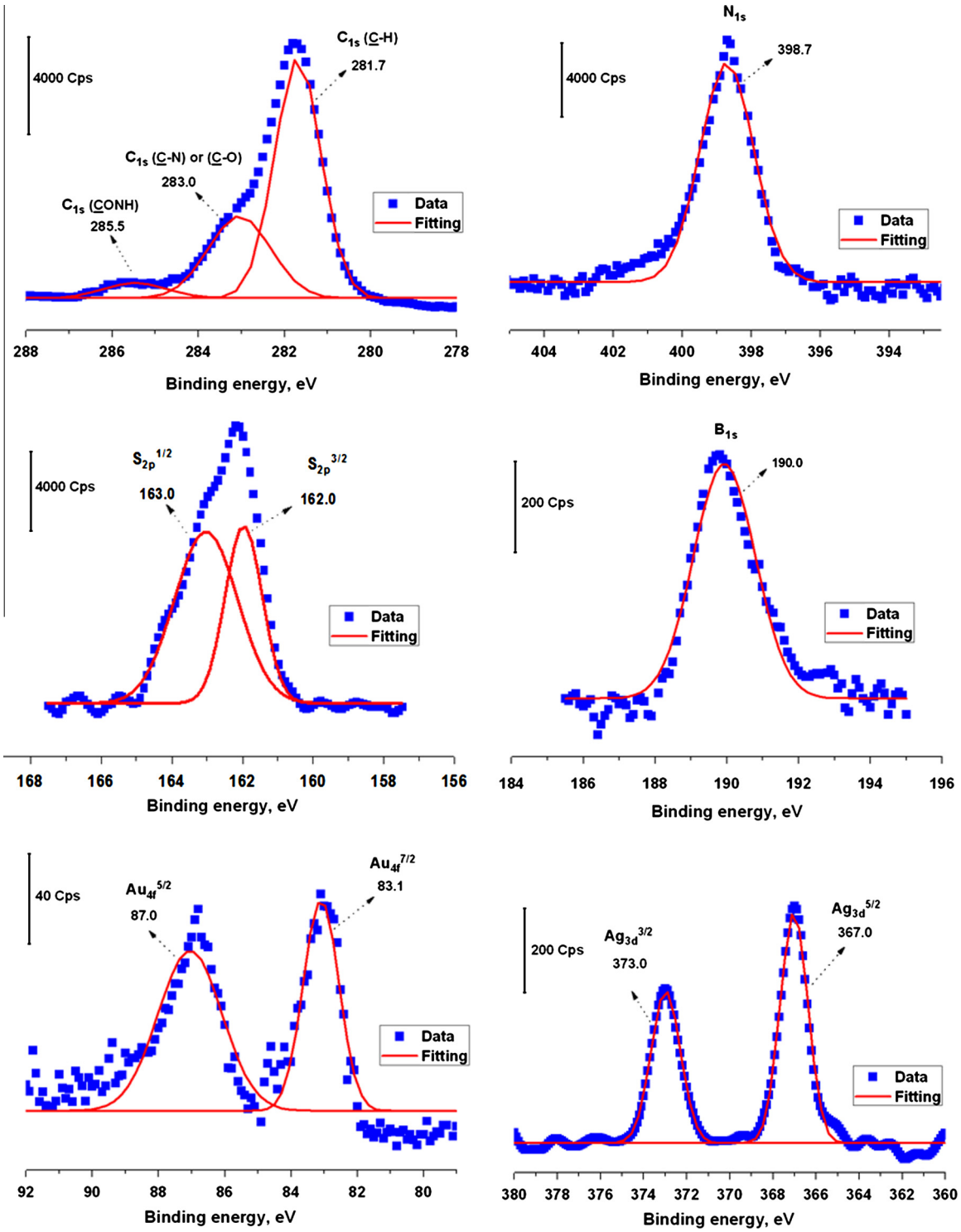

Fig. 2. The narrow region of XPS spectra of the nanocomposite for the deconvolution spectra of the C1s, N1s, B1s, Au4f, and Ag3d.

spectra are shown in Fig. 2. The C_{1s}, N_{1s}, B_{1s}, Au_{4f}, and Ag_{3d} spectra indicate the formation of the MBA–Ag@AuNPs–GO nanocomposite. The C_{1s} core-level spectra of the MBA–Ag@AuNPs–GO nanocomposite were curve-fitted in Fig. 2. The peaks at 281.7 eV, 283.0 eV, and 285.7 eV are assigned to CH, CN, and CONH, respectively [47–49]. The peak located at 398.7 eV in the N_{1s} narrow region is assigned to C–N groups in the covalent attachment of the carboxyl group of the GO with the amino group of the ATP [47]. S_{2p} region was curve-fitted with two components by a doublet ($2p^{1/2}$ and $2p^{3/2}$) due to the spin-orbit coupling. It is thought that the peak observed at 163.0 eV indicates that the sulfur atom in the nanocomposite was grafted with the AuNPs. The peak at 162.0 eV can be assigned to free mercapto group in unreacted ATP. The peak signal at 83.0 eV indicated the functionalization of Au with sulfur [50]. Ag_{3d} region is characterized by a doublet $3d^{5/2}$ and $3d^{3/2}$ signals at 367.0 and 373.0 eV, respectively, corresponding to the presence of Ag° [50]. The peak observed at about 190 eV is assigned to the B–C bond [1,51]. The successful synthesis

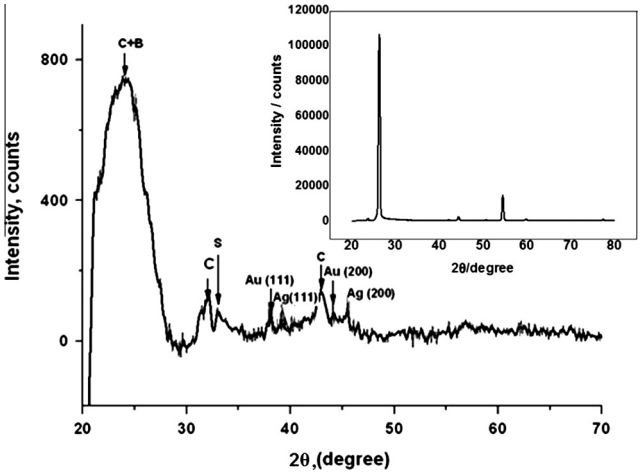

Fig. 3. XRD patterns of the nanocomposite (inset: the XRD patterns of graphite).

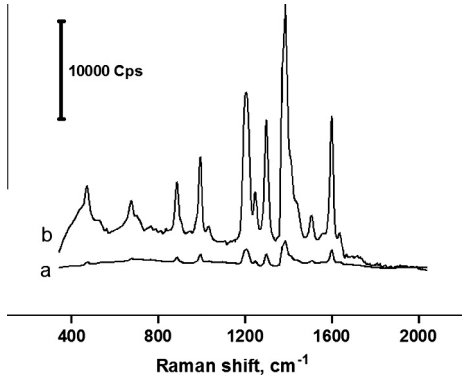

Fig. 4. Raman spectra of (a) the ATP functionalized GO and (b) the Ag@AuNPs–GO nanocomposite.

of the nanocomposite is also confirmed by XRD measurements. The XRD patterns of the graphite and as-synthesized MBA–Ag@AuNPs–GO nanocomposite are shown in Fig. 3. As seen in the inset of Fig. 3, the XRD patterns show a very intense and narrow peak at $2\theta = 26.5°$ corresponding to the (002) planes of GO layers. The weak peaks at $2\theta = 44.6°$ and $2\theta = 54°$ corresponded to (101) and (004) planes of GO layers, respectively [52]. In Fig. 3, a broad peak at $2\theta = 20–28°$ confirms that the structure expansion as oxygen-containing groups incorporates between the carbon sheets during the course of strong oxidation. The formations of Au° and Ag° were confirmed by $2\theta = 38.5°$ and 44.6° peaks, which indicate the (111) and (200) crystalline planes of Au°, and by $2\theta = 39.3°$ and 45.2° peaks, which indicate the (111) and (200) crystalline planes of Ag° [53–75].

The ATP functionalized GO and Ag@AuNPs–GO nanocomposites were also characterized by using a Raman Microscopy (DeltaNu Examiner Raman Microscopy system). The Raman spectra of the ATP functionalized GO and Ag@AuNPs–GO nanocomposites are shown in Fig. 4. The bands at 890 cm^{-1} and 1340 cm^{-1} are assigned to the C–COO^- stretching vibration and COO^- symmetric stretching vibration, respectively. The bands at 665 cm^{-1} and 474 cm^{-1} can be assigned to C–S stretching vibrations of the probe, which indicate that thiol group reacts with the AuNPs [50]. The amide band is very weak and appears in the range of 1500–1550 cm^{-1} in the Raman spectra of the ATP functionalized GO [50]. A strong and reliable SERS signal has been detected in the Ag@AuNPs–GO nanocomposite. As seen from the Raman spectra of the Ag@AuNPs–GO, Ag@AuNPs can be used to increase Raman signal intensities dramatically for the ATP functionalized GO that does not get the significant Raman signals.

3.2. Optimization of the experimental conditions

The experimental parameters for the determination of glucose were optimized with regard to reaction time, concentration of MBA, and reaction temperature. Fig. 5a demonstrates that the SERS signal increases up to 35 °C and then gradually decreases. It is thought that the MBA film is not stable at temperatures higher than 35 °C. Hence, the optimized temperature was chosen as 35 °C. In terms of probe preparation, the most suitable concentration of MBA was 20.0 mM for the determination of glucose (Fig. 5b). The Raman spectra were obtained with an increasing reaction time after immobilization of glucose in MBA–Ag@AuNPs–GO film. The SERS signal increases up to 15 min, and then, the SERS response decreases and stays almost constant, as shown in Fig. 5c. Thus, we chose 15 min as optimum reaction time.

3.3. Detection of glucose at MBA–Ag@AuNPs–GO film using SERS

Fig. 6a demonstrates the SERS spectra containing different concentrations of glucose. All the SERS spectra of solutions containing

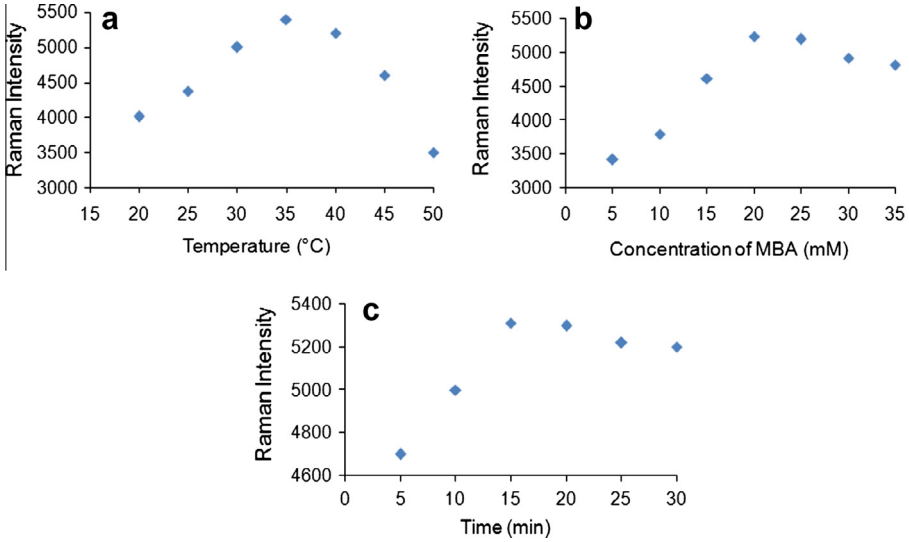

Fig. 5. Optimization of experimental parameters: effect of (a) temperature, (b) concentration of MBA, and (c) reaction time (for 2.0 mM glucose).

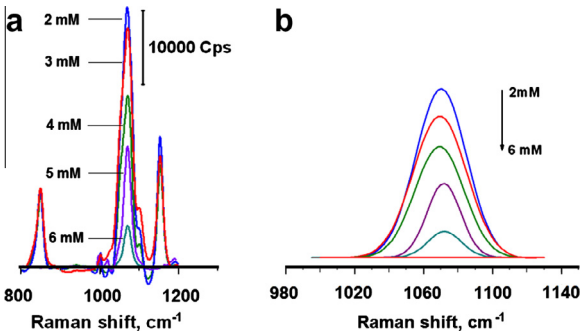

Fig. 6. Symmetric B–O stretching bands of (a) MBA–Ag@AuNPs–GO nanocomposite after complexation with glucose and (b) curve-fitting of the Raman shift of the MBA–Ag@AuNPs–GO: In the presence of different concentrations of range from 2 mM to 6 mM GOD.

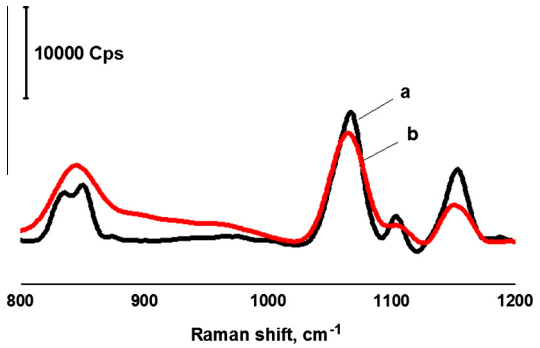

Fig. 7. Raman spectra of (a) standard glucose solution of 2.0 mg/mL and (b) 2.0 mg/mL glucose solution containing the proteins such as HAS, C3, and transferrin.

Table 1
Data of the calibration curves for the proposed method (n = 6).

Regression equation	$y = -7355.6x + 7672$
Standard error of the slope	0.44
Standard error of the intercept	0.69
Correlation coefficient (R^2)	0.9930
Linearity range (mM)	2.0–6.0
Number of data points	5
LOD (mM)	0.33
LOQ (mM)	1

$y = ax + b$; y: Raman intensity, x: glucose concentration (mM), a: slope, b: intercept. LOQ: Limit of quantification, LOD: Limit of detection.

different concentrations of glucose immobilized into MBA–Ag@AuNPs–GO nanocomposite were corrected by the blank solution containing mercaptophenyl boronic acid terminated Ag@AuNPs/graphene oxide nanomaterial. The boronic acid groups of the nanomaterial in the blank solution are not in complexation with diol groups of glucose. The SERS spectrum of the blank solution was subtracted from the SERS spectra of the mercaptophenyl boronic acid terminated Ag@AuNPs/graphene oxide nanocomposite. The SERS spectra of MBA–Ag@AuNPs–GO were fitted by using Origin Pro. 7.5 and are shown in Fig. 6b. The SERS peak of B–O stretch at 1070 cm^{-1} was utilized for assessment of glucose amount (as shown in Fig. 6b). The data of calibration curves are given in Table 1. So, the concentration of glucose in blood samples was calculated to be 1.97 ± 0.002 mM for six times repeated measurements. Therefore, the Ag@AuNPs–GO nanocomposite is used as a novel glucose sensor. The reproducibility of the developed biosensor was also investigated using 2.0 mM glucose. The relative standard deviation (RSD) was 2.9% with a series of six experiments. These results indicated that the MBA–Ag@AuNPs–GO film ensures suitable microenvironment for GOD to perform SERS activity.

The long-time stability of the developed biosensor was explored over 30 days. The Ag@AuNPs–GO nanocomposite was stored at 4 °C. The nanocomposite was used for the analysis of 2.0 mM glucose every 3 days. The obvious change in SERS spectrum of 2.0 mM glucose immobilized into MBA–Ag@AuNPs–GO nanocomposite was not observed over this period. So, we can say that the developed biosensor had good stability.

3.4. Selectivity

To investigate the selectivity of the analytical system, the influence of several proteins was studied. 200 μL of MBA–Ag@AuNPs–GO solution was immediately added into the mixture of 10 μL of 40 mM glucose in citrate buffer (0.1 M, pH 5.0) and 10 μL of 60 mg/mL BSA solution. Hence, about 3.0 mg/mL BSA solution was obtained. After stirring at room temperature for 15 min, SERS spectrum of the final solution was recorded. The decrease in SERS signal caused by the addition of BSA at 1070 cm^{-1} was negligible. The effects of 10.0 mg/mL HAS, 1.0 mg/mL C3, and 1.0 mg/mL transferrin were evaluated by the same way. The significant change in SERS spectrum is not observed (Fig. 7). So, glucose was selectively detected in the presence of the other proteins by means of SERS.

In addition, the recovery experiments were performed with different glucose concentrations (3.0, 4.0, and 5.0 mM glucose). The results are presented in Table 2. Closeness of the results to 100.00% showed that recovery of the developed biosensor was very good.

Table 2
The recoveries of glucose in blood samples (n = 6).

Added glucose (mM)	Found glucose (mM)	Recovery (%)	RSD
3.0	2.9 ± 0.02	96.67	4.1
4.0	3.8 ± 0.04	95.00	2.7
5.0	5.2 ± 0.05	104.00	3.1

4. Conclusion

In this study, a novel glucose biosensor was developed on mercaptophenyl boronic acid terminated Ag@AuNPs/graphene oxide nanomaterials. The developed biosensor exhibited a linear range of glucose detection between 2.0 and 6.0 mM, and the detection limit was 0.33 mM. The developed glucose biosensor was successfully applied to human blood sample. It could provide high selectivity in the presence of proteins. Thus, compared to the other analytical methods, the SERS method can offer a number of advantages such as selectivity, high speed of analysis, and cost-effectiveness.

Acknowledgment

The authors are grateful for the financial support provided by The Scientific and Technological Research Council of Turkey; Project Number: 111T983.

References

[1] D. Das, D.M. Kim, D.S. Park, Y.B. Shim, Electroanalysis 23 (2011) 2036.
[2] K. Morita, N. Hirayama, H. Imura, A. Yamaguchi, N. Teramae, J. Electroanal. Chem. 656 (2011) 192.
[3] C.S. Shan, H.F. Yang, D.X. Han, Q.X. Zhang, A. Ivaska, L. Niu, Biosens. Bioelectron. 25 (2010) 1070.
[4] Y.W. Zhang, S. Liu, L. Wang, X.Y. Qin, J.Q. Tian, W.B. Lu, G.H. Chang, X.P. Sun, Rsc. Adv. 2 (2012) 538.

[5] B.Y. Wu, S.H. Hou, F. Yin, Z.X. Zhao, Y.Y. Wang, X.S. Wang, Q. Chen, Biosens. Bioelectron. 22 (2007) 2854.
[6] Y.C. Tsai, S.C. Li, J.M. Chen, Langmuir 21 (2005) 3653.
[7] P.C. Chen, L.S. Wan, B.B. Ke, Z.K. Xu, Langmuir 27 (2011) 12597.
[8] W.T. Wu, N. Mitra, E.C.Y. Yan, S.Q. Zhou, ACS Nano 4 (2010) 4831.
[9] K. Kneipp, H. Kneipp, I. Itzkan, R.R. Dasari, M.S. Feld, Curr. Sci. India 77 (1999) 915.
[10] C.L. Haynes, A.D. McFarland, R.P. Van Duyne, Anal. Chem. 77 (2005) 338a.
[11] P. Etchegoin, R.C. Maher, L.F. Cohen, H. Hartigan, R.J.C. Brown, M.J.T. Milton, J.C. Gallop, Chem. Phys. Lett. 375 (2003) 84.
[12] P. Vandenabeele, H.G.M. Edwards, L. Moens, Chem. Rev. 107 (2007) 675.
[13] M. Seydack, Biosens. Bioelectron. 20 (2005) 2454.
[14] O. Lyandres, J.M. Yuen, N.C. Shah, R.P. VanDuyne, J.T. Walsh, M.R. Glucksberg, Diabetes Technol. 10 (2008) 257.
[15] D.A. Stuart, C.R. Yonzon, X.Y. Zhang, O. Lyandres, N.C. Shah, M.R. Glucksberg, J.T. Walsh, R.P. Van Duyne, Anal. Chem. 77 (2005) 4013.
[16] C.L. Haynes, C.R. Yonzon, X.Y. Zhang, R.P. Van Duyne, J. Raman Spectrosc. 36 (2005) 471.
[17] K.E. Shafer-Peltier, C.L. Haynes, M.R. Glucksberg, R.P. Van Duyne, J. Am. Chem. Soc. 125 (2003) 588.
[18] C.R. Yonzon, C.L. Haynes, X.Y. Zhang, J.T. Walsh, R.P. Van Duyne, Anal. Chem. 76 (2004) 78.
[19] U.S. Dinish, F.C. Yaw, A. Agarwal, M. Olivo, Biosens. Bioelectron. 26 (2011) 1987.
[20] G. Mattei, L.G. Quagliano, M. Pagannone, Europhys. Lett. 11 (1990) 373.
[21] Y.J. Oh, K.H. Jeong, Adv. Mater. 24 (2012) 2234.
[22] J. Cejkova, V. Prokopec, S. Brazdova, A. Kokaislova, P. Matejka, F. Stepanek, Appl. Surf. Sci. 255 (2009) 7864.
[23] L.A.F. Costa, H.S. Breyer, J.C. Rubim, Vib. Spectrosc. 54 (2010) 103.
[24] G.M. Herrera, A.C. Padilla, S.P. Hernandez-Rivera, Nanomaterials 3 (2013) 158.
[25] J. Baniukevic, I.H. Boyaci, A.G. Bozkurt, U. Tamer, A. Ramanavicius, A. Ramanaviciene, Biosens. Bioelectron. 43 (2013) 281.
[26] S. Stankovich, D.A. Dikin, G.H.B. Dommett, K.M. Kohlhaas, E.J. Zimney, E.A. Stach, R.D. Piner, S.T. Nguyen, R.S. Ruoff, Nature 442 (2006) 282.
[27] J.C. Meyer, A.K. Geim, M.I. Katsnelson, K.S. Novoselov, T.J. Booth, S. Roth, Nature 446 (2007) 60.
[28] J.L. Vickery, A.J. Patil, S. Mann, Adv. Mater. 21 (2009) 2180.
[29] C. Xu, X. Wang, J.W. Zhu, J. Phys. Chem. C 112 (2008) 19841.
[30] B. Seger, P.V. Kamat, J. Phys. Chem. C 113 (2009) 7990.
[31] Y.C. Xin, J.G. Liu, X. Jie, W.M. Liu, F.Q. Liu, Y. Yin, J. Gu, Z.G. Zou, Electrochim. Acta 60 (2012) 354.
[32] E. Yoo, J. Kim, E. Hosono, H. Zhou, T. Kudo, I. Honma, Nano Lett. 8 (2008) 2277.
[33] M.D. Stoller, S.J. Park, Y.W. Zhu, J.H. An, R.S. Ruoff, Nano Lett. 8 (2008) 3498.
[34] J. Zhang, J.G. Yu, M. Jaroniec, J.R. Gong, Nano Lett. 12 (2012) 4584.
[35] Q.J. Xiang, J.G. Yu, M. Jaroniec, J. Am. Chem. Soc. 134 (2012) 6575.
[36] Q.J. Xiang, J.G. Yu, M. Jaroniec, Chem. Soc. Rev. 41 (2012) 782.
[37] Q.J. Xiang, J.G. Yu, J. Phys. Chem. Lett. 4 (2013) 753.
[38] S.J. He, B. Song, D. Li, C.F. Zhu, W.P. Qi, Y.Q. Wen, L.H. Wang, S.P. Song, H.P. Fang, C.H. Fan, Adv. Funct. Mater. 20 (2010) 453.
[39] S. Niyogi, E. Bekyarova, M.E. Itkis, J.L. McWilliams, M.A. Hamon, R.C. Haddon, J. Am. Chem. Soc. 128 (2006) 7720.
[40] Z.B. Liu, Y.F. Xu, X.Y. Zhang, X.L. Zhang, Y.S. Chen, J.G. Tian, J. Phys. Chem. B 113 (2009) 9681.
[41] Y. Yang, Y.M. Zhang, Y. Chen, D. Zhao, J.T. Chen, Y. Liu, Chem. – Eur. J. 18 (2012) 4208.
[42] X.X. Ma, H.Q. Tao, K. Yang, L.Z. Feng, L. Cheng, X.Z. Shi, Y.G. Li, L. Guo, Z. Liu, Nano Res. 5 (2012) 199.
[43] M.H. Ullah, K. Il, C.S. Ha, Mater. Lett. 60 (2006) 1496.
[44] W.S. Hummers, R.E. Offeman, J. Am. Chem. Soc. 80 (1958) 1339.
[45] S.F. Hou, S.J. Su, M.L. Kasner, P. Shah, K. Patel, C.J. Madarang, Chem. Phys. Lett. 501 (2010) 68.
[46] A.P. Tuan, B.C. Choi, K.T. Lim, Y.T. Jeong, Appl. Surf. Sci. 257 (2011) 3350.
[47] F. Montagne, J. Polesel-Maris, R. Pugin, H. Heinzelmann, Langmuir 25 (2009) 983.
[48] R. Schlapak, P. Pammer, D. Armitage, R. Zhu, P. Hinterdorfer, M. Vaupel, T. Fruhwirth, S. Howorka, Langmuir 22 (2006) 277.
[49] E. Bekyarova, M.E. Itkis, P. Ramesh, C. Berger, M. Sprinkle, W.A. de Heer, R.C. Haddon, J. Am. Chem. Soc. 131 (2009) 1336.
[50] R. Guzel, Z. Ustundag, H. Eksi, S. Keskin, B. Taner, Z.G. Durgun, A.A.I. Turan, A.O. Solak, J. Colloid Interf. Sci. 351 (2010) 35.
[51] D. Barriet, C.M. Yam, O.E. Shmakova, A.C. Jamison, T.R. Lee, Langmuir 23 (2007) 8866.
[52] P. Bradder, S.K. Ling, S.B. Wang, S.M. Liu, J. Chem. Eng. Data 56 (2011) 138.
[53] G.I. Titelman, V. Gelman, S. Bron, R.L. Khalfin, Y. Cohen, H. Bianco-Peled, Carbon 43 (2005) 641.
[54] A.S. Lanje, S.J. Sharma, R.B. Pode, J. Chem. Pharm. Res. 2 (2010) 478–483.
[55] R.N. Goyal, V.K. Gupta, N. Bachheti, R.A. Sharma, Electroanalysis 20 (2008) 757–764.
[56] V.K. Gupta, A.K. Jain, P. Kumar, Sens. Actuat. B 120 (2006) 259–265.
[57] V.K. Gupta, A.K. Jain, P. Kumar, S. Agarwal, G. Maheshwari, Sens. Actuat. B 113 (2006) 182–186.
[58] R.N. Goyal, V.K. Gupta, S. Chatterjee, Biosensors and Bioelectronics 24 (2009) 1649–1654.
[59] V.K. Gupta, A.K. Jain, G. Maheshwari, H. Lang, Sens. Actuat. B 117 (2006) 99–106.
[60] V.K. Gupta, R. Prasad, A. Kumar, Talanta 60 (2003) 149–160.
[61] V.K. Gupta, S. Chandra, R. Mangla, Electrochim. Acta. 47 (2002) 1579–1586.
[62] R.N. Goyal, V.K. Gupta, N. Bachheti, Anal. Chim. Acta. 597 (2007) 82–89.
[63] V.K. Gupta, R. Jain, K. Radhapyari, N. Jadon, S. Agarwal, Analytical Biochemistry 408 (2011) 179–196.
[64] R.N. Goyal, V.K. Gupta, S. Chatterjee, Biosensors and Bioelectronics 24 (2009) 3562–3568.
[65] V.K. Gupta, A.K. Singh, S. Mehtab, B. Gupta, Anal. Chim. Acta. 566 (2006) 5–10.
[66] V.K. Gupta, A.K. Singh, M. Al Khayat, B. Gupta, Anal. Chim. Acta. 590 (2007) 81–90.
[67] V.K. Gupta, S. Chandra, H. Lang, Talanta 66 (2005) 575–580.
[68] R.N. Goal, V.K. Gupta, S. Chatterjee, Electrochimica Acta. 53 (2008) 5354–5360.
[69] V.K. Gupta, Tawfik A, Saleh, Water Research 45 (2011) 2207–2212.
[70] V.K. Gupta, B. Gupta, A. Rastogi, S. Agarwal, A. Nayak, J. Hazard. Mater. 186 (2011) 891–901.
[71] V.K. Gupta, A. Mittal, A. Malviya, J. Mittal, J. Colloid Interface Sci. 355 (2009) 24–33.
[72] V.K. Gupta, A. Rastogi, J. Colloid Interface Sci. 342 (2010) 533–539.
[73] V.K. Gupta, R.N. Goyal, R.A. Sharma, Anal. Chim. Acta 647 (2009) 66–71.
[74] R.N. Goyal, V.K. Gupta, A. Sangal, N. Bachheti, Electroanalysis 17 (2005) 2217–2223.
[75] R.N. Goyal, M. Oyama, V.K. Gupta, S.P. Singh, S. Chatterjee, Sensors Actuators:B. Chem. 134 (2008) 816–821.